

Cite this: *RSC Adv.*, 2015, 5, 84879

# Highly transparent poly(2-ethyl-2-oxazoline)-TiO<sub>2</sub> nanocomposite coatings for the conservation of matte painted artworks†

A. Colombo,<sup>\*ab</sup> F. Gherardi,<sup>c</sup> S. Goidanich,<sup>c</sup> J. K. Delaney,<sup>d</sup> E. R. de la Rie,<sup>e</sup>  
M. C. Ubaldi,<sup>b</sup> L. Toniolo<sup>c</sup> and R. Simonutti<sup>a</sup>

A nanocomposite coating based on TiO<sub>2</sub> nanoparticles and poly(2-ethyl-2-oxazoline) is used as consolidant of matte painted surfaces (temperas, watercolors, modern paintings). The aim of this work is to provide advances in the conservation of these works of art, while preserving their optical appearance, in terms of colour and gloss. Fiber Optic Reflectance Spectroscopy (FORS) measurements of a painting-model (an acrylic black monochrome) treated with the nanocomposite coatings revealed that it is possible to match the optical appearance of the painted surface by tuning the amount of nanoparticles in the polymeric matrix. The requirement of retreatability of the material has been verified by removing the nanocomposite cast on the painted surface with aqueous solutions. FTIR and SEM/EDX measurements showed that almost no traces of the nanocomposite remained on the painted surface, allowing its use for the treatment of real paintings. Tests were performed using a contemporary studio-model on canvas attributed to Agostino Bonalumi (1935–2013).

Received 8th June 2015  
Accepted 29th September 2015

DOI: 10.1039/c5ra10895k

[www.rsc.org/advances](http://www.rsc.org/advances)

## Introduction

One of the most important aims of the conservation and restoration of cultural heritage is the preservation of the original materials. A common treatment is that of consolidation, which consists of the deposition of a suitable material, often a polymer, among cracked or flaking layers of painted surfaces. This treatment is one of the most delicate operations because it may be invasive from the chemical and aesthetical points of view. A first concern is that of aging of the added material and interaction with the original materials, since complete removability after the application is not always possible. Another concern is that of change of the original appearance of the work of art, in terms of gloss and colour saturation. Moreover, consolidation treatments are often localized in degraded areas, implying a loss of optical homogeneity.

This is less of a concern in the case of many old master paintings, which typically are covered with a final transparent

layer, called varnish, which provides a homogeneous appearance. Such paintings are optically less affected by consolidation treatments. The effects of varnishes on the appearance of paintings have been extensively studied and, generally speaking, varnishing results in increased gloss and colour saturation.<sup>1–3</sup> With the advent of Impressionism in the late 19<sup>th</sup> century, the use of varnish started to decline, and paintings were often left matte. Conservation treatments of such paintings (Impressionist, Macchiaioli, Spazialist, American realist are only some examples of artist movements with this preference) are challenging, as materials added to re-adhere or consolidate fragile and flaking painted layers tend to change their appearance. Varnishing such paintings is generally discouraged as the optical appearance of the artwork may be altered. The same is true for consolidating treatments of such paintings, which may have dramatic effects on their appearance. Until now, a satisfactory solution to this problem has not been found and in the more demanding cases, such as the conservation of dark monochromes, conservators avoid treating their paint layers because many treatments would induce a change of the surface appearance, in terms of colour and gloss.

Nanotechnology has been used with promising results for the conservation of cultural heritage. As an example the consolidation of wall painting and the de-acidification of the paper with calcium and magnesium hydroxides nanoparticles have been reported.<sup>4–8</sup> Recently, also titanium dioxide nanoparticles played an important role in the cleaning of stones, as self-cleaning coating for its well-known photocatalytic<sup>9–13</sup> and anti-bacterial activity.<sup>14</sup> On the other hand, TiO<sub>2</sub> is

<sup>a</sup>Department of Materials Science, University of Milano-Bicocca, via R. Cozzi 53, 20125, Milano, Italy. E-mail: [annalisa.colombo@fondazionecef.it](mailto:annalisa.colombo@fondazionecef.it)

<sup>b</sup>CIFE Foundation, via G. Colombo 81, 20133, Milano, Italy

<sup>c</sup>Chemistry, Material and Chemical Engineering Department "G. Natta", Politecnico di Milano, via Mancinelli 7, 20131, Milano, Italy

<sup>d</sup>Scientific Research Department, National Gallery of Art, Washington, D. C., 20565, USA

<sup>e</sup>University of Amsterdam, Conservation & Restoration, Johannes Vermeerplein 1, 1071, DV Amsterdam, The Netherlands

† Electronic supplementary information (ESI) available. See DOI: 10.1039/c5ra10895k

a semiconductor oxide ( $E_g \approx 3$  eV), transparent in the visible range, with a high refractive index (2.49 at 589 nm for anatase phase),<sup>15</sup> so it meets several requirements for important applications in optoelectronics,<sup>16</sup> photovoltaics,<sup>17</sup> and catalysis fields.<sup>18–20</sup> Optical properties of synthetic polymers, such as UV absorption,<sup>21</sup> diffusion,<sup>22</sup> and refractive index<sup>23</sup> can be improved and modulated by the introduction of TiO<sub>2</sub> nanoparticles in the organic matrix, preserving the material transparency, the absence of colour, lightness and flexibility. There are not many inorganic nanoparticles with the same optical properties of TiO<sub>2</sub> (high refractive index, transparency in the visible with UV absorption). Some high refractive index polymer nanocomposites reported in literature were prepared with ZrO<sub>2</sub> ( $n = 2.16$  at 589 nm)<sup>24</sup> and ZnO ( $n = 2.00$  at 589 nm)<sup>25</sup> that, like TiO<sub>2</sub>, show also photocatalytic properties.<sup>26</sup> Moreover, TiO<sub>2</sub> is most often used as inorganic phase due to the higher refractive index and its easier preparation in both laboratory and industry.<sup>27</sup>

Here we report a proof-of-concept of innovative coatings, based on TiO<sub>2</sub> nanoparticles and poly(2-ethyl-2-oxazoline) (PEOX), able to mimic the surface diffusive properties of matte painted surfaces. PEOX is a material already used in the conservation field as adhesive and consolidant, but seldom on painted surfaces.<sup>28–32</sup> In PEOX films containing TiO<sub>2</sub> nanoparticles, surface and volume scattering are a function of the nanoparticles' concentration in the polymeric matrix; however high optical transparency is always preserved. These films, starting from a PEOX aqueous solution containing TiO<sub>2</sub> nanoparticles, have been applied on painted specimens realized by using a commercial acrylic colour brushed on an industrial canvas, as a model for modern paintings characterized by a matte appearance. The ability of these films to coat the painted surface without changing its optical properties has been evaluated using Fiber Optics Reflectance Spectroscopy (FORS), which measured the diffuse reflectance spectrum from a surface in the visible to near infrared (350 to 2500 nm). The chemical stability and removability of the coatings were studied using accelerated aging, infrared spectroscopy and electron microscopy.

## Experimental section

### Materials

TiO<sub>2</sub> nanoparticles are elongated clusters whose the longest axis measures about 40 nm composed of primary nanocrystals of about 5–6 nm diameter. They were synthesized according to the non-aqueous route<sup>33</sup> as reported in a previous work.<sup>34</sup> PEOX (Aquazol 200®, Polymer Chemistry Innovation,  $M_w = 200000$ , purchased from CTS s.r.l.) film (A0) was prepared by evaporation of the water and used as reference. The polymer was used as received. Nanocomposite films were obtained by mixing different ratios of the nanoparticles dispersion in the aqueous polymeric solution. Films based on an increasing concentration of nanoparticles in the polymeric matrix: 16 wt%, 28 wt% and 44 wt%, called C16, C28, C44 respectively, were prepared by evaporation of the solvent at room temperature and environmental pressure. Aqueous dispersions and the solution of pure polymer were cast on painting-model surfaces.

The painting-model was obtained by casting an acrylic black colour (bone black, Windsor and Newton® tube) on a pre-prepared cotton canvas. The aim is to simulate a black monochrome painting, one of the most difficult cases in conservation treatments. Painting-replicas were treated with nanocoatings by brushing them on the black surface. Every replica was coated with the same amount in weight of material. The same treatment has been performed on the studio-model attributed to Agostino Bonalumi (1935–2013).

Removal of nanocomposite films has been carried out by using two tampons soaked in polysorbate surfactant TWEEN 20 (CTS s.r.l.) and a water solution of ammonium citrate tribasic (TAC) (CTS s.r.l.) 1 wt%, two years after the treatment. These specimens were kept in a conservation studio, in front of a window facing west, exposed to a measured illuminance coming from sunlight of about  $47 \pm 5$  lux, in good agreement with museum lighting guidelines.<sup>35</sup> The quantification of the flux was performed by using a portable digital lux-meter (La Fayette DT1300), at about 01 : 00 p.m., in winter.

### Characterization techniques

Ellipsometric measurements were carried out on glass substrates treated with the nanocomposite coatings, by means of a variable angle spectroscopic ellipsometer WVASE32 (J. Woollam). All measurements were done at three angles of incidence: 50°, 55° and 60°; the operating wavelengths range is between 300 to 1700 nm. Nanocomposite films were considered as transparent dielectrics and the refractive index dispersion has been described by the Cauchy parameterization model ( $n(\lambda) = A + B/\lambda^2 + C/\lambda^4$ ).<sup>15</sup> This model has been used for fitting ellipsometric data. In order to verify the surface roughness Bruggeman Effective Medium Approximation (EMA) has been used; this model consists of a homogenous mixture of material and voids.<sup>36</sup> As consequence, the stack model used for analyzing the samples is characterized by three layers: glass, film, film + voids (EMA).

Nanocomposite coatings cast on microscope glass were artificially aged in a xenon arc Weather-ometer (Atlas). The Weather-ometer irradiance was set to  $0.9 \text{ W m}^{-2}$  at 420 nm using a xenon arc lamp (6500 watt) with an inner soda lime and outer borosilicate filter in order to simulate indoor conditions. The corresponding illuminance was about 75 000 lux. The temperature and humidity was maintained at 25 °C and  $45 \pm 6\%$  RH. In order to avoid the reflection of the light, a black cardboard was set on the back of the samples.

The accelerated aging was performed to speed up the natural aging process of the studied material (two years when this paper was written). Artificial aging tests are often used in the cultural heritage field to predict the long-term effect of a conservation treatment. Thus, its value is to predict some effects or reactions that can contribute to the deterioration of materials or conservation treatments, in relative terms.<sup>37</sup>

Our interest is using artificial aging to identify the photocatalytic effects of the TiO<sub>2</sub> nanoparticles on the polymer matrix.

The aging of the materials was followed with Micro-Attenuated Total Reflection (ATR) Fourier Transform Infrared

(FTIR) spectroscopy and Gel Permeation Chromatography (GPC). FTIR analyses were carried out with a Nicolet 6700 spectrophotometer coupled with a Nicolet Continuum FTIR microscope equipped with a MCT detector (acquired between 4000 and 600  $\text{cm}^{-1}$  with 256 acquisitions and 8  $\text{cm}^{-1}$  resolution) with an attenuated total reflection Si crystal accessory (ATR). GPC analyses were performed with a Perkin-Elmer (PE) liquid Chromatography system consisting of PE Series 410 LC pump, two Polymer Laboratories PL-gel 5  $\mu\text{m}$  mixed D-columns (300 mm  $\times$  7.5 mm) and a Millipore 410 differential refractometer. The columns and refractometer were maintained at 35  $^{\circ}\text{C}$ . Tetrahydrofuran (THF) was used as the eluant (1 ml  $\text{min}^{-1}$ ). The instrument was calibrated daily using five polystyrene standards with weight-average molecular weights ( $M_w$ ) ranging between 162 and 207 000. GPC samples were prepared by dissolving the polymer in unstabilized THF (up to 1% in weight); in the case of nanocoatings, the polymer was collected after the nanoparticles precipitation in THF.

The chemical composition of the industrial black tube colour was valued with a Q500 Thermogravimetric analyzer (TA Instrument). The sample was heated to 800  $^{\circ}\text{C}$  in nitrogen atmosphere.

The painting-model was optically characterized with a fiber-optic spectroradiometer, FS3 (ASD Inc, Boulder, CO) for obtaining FORS (Fibers Optics Reflectance Spectroscopy) spectra at various sites. The spectrometer operated from 350 nm to 2500 nm with a spectral sampling of 1.4 nm from 350 to 1000 nm and 2 nm from 1000 to 2500 nm. The spectral resolution at 700 nm was 3 nm, and at 1400 and 2100 nm it was 10 nm. The light source of a leaf probe head (ASD Inc) was used at a distance of 10 cm in order to briefly illuminate the painting (4000 lux), and the fiber was placed  $\sim 1$  cm from the object, giving a  $\sim 3$  mm spot size to the painting. The samples were illuminated at 45 degrees and the light collected normal to the sample. Typically 64 spectra were averaged and total acquisition time was 7 s per point. Through the integration of the reflectance spectra in the visible range (380–720 nm) the determination of the samples colours in the CIE (Commission International de L'Eclairage)- $L^*$ ,  $a^*$ ,  $b^*$  colour space was performed. Calculations were performed using the CIE Standard Illumination D65, based on actual spectral measurements of the daylight and a correlated colour temperature of 6504 K. This is the most widely used colour temperature in the industry of graphic arts and in the field of cultural heritage, where it is employed to check colour changes in works of art. The colour differences are generally calculated as the square root of the combined squares of the chromaticity differences ( $a^*$ ,  $b^*$ ,  $L^*$ ) and is defined as delta error ( $\Delta E$ ):

$$\Delta E = \sqrt{(a^*)^2 + (b^*)^2 + (L^*)^2}$$

$\Delta E$  has to be higher than 1.0 so that the changes of colours are perceptible by human eyes.

The chemical stability of the nanocomposite films cast on the painted replicas preserved in a conservation studio, in front of a window facing west, was monitored by Micro-ATR FTIR.

FTIR analyses were carried out with a Nicolet 6700 spectrophotometer coupled with a Nicolet Continuum FTIR microscope equipped with a MCT detector (acquired between 4000 and 600  $\text{cm}^{-1}$  with 128 acquisitions and 4  $\text{cm}^{-1}$  resolution) with an attenuated total reflection Ge crystal accessory (ATR). The spectra were baseline corrected and subtracted using Omnic software, and normalized on the intensity of the  $\text{CH}_3$  bending vibration (at 1374  $\text{cm}^{-1}$ ), which is the most stable band in terms of intensity.

The efficiency of the removal process of nanocomposite coatings from the painted surface was investigated using Micro-ATR FTIR, as well as Environmental Scanning Electron Microscopy (ESEM) observations and Energy Dispersive X-ray (EDX) analyses, performed using a Zeiss EVO 50 EP ESEM, equipped with an Oxford INCA 200 – Pentafet LZ4 spectrometer. EDX technique was used to obtain a semi-quantitative evaluation of Ti atoms present on the treated and cleaned painted surface, relative to the other elements identified in the spectrum (C, O, Na, Si, P, S, K, Ca), by opportunely converting the area under the peak into number percent. The instrument detection limit is 0.03%.

VIS spectrophotometric measurements of the real painting were carried out with a Konica Minolta CM-600D instrument, with a D65 illuminant at 8 $^{\circ}$ , wavelength range between 360 nm and 740 nm. Measurements were elaborated according to the CIE  $L^*$ ,  $a^*$ ,  $b^*$  standard colour system: ten measurements were performed on each area and the average results of  $L^*$ ,  $a^*$ ,  $b^*$  were used to calculate the colour difference  $\Delta E$  between naturally aged and unaged films. Optical inspection of the real painting surface before and after the conservation treatment with nanocoatings was performed with a portable digital microscope Dino-Lite Premiere AM7013MT, colour CMOS sensor and white LED illuminator.

## Results and discussion

### Optical properties of nanocoatings cast on a painting-model

As described in the literature, the gloss of paints is a function of pigment volume concentration (PVC);<sup>38</sup> in general, the maximum gloss is achieved when the amount of binder is sufficient to cover all the pigment particles (the critical pigment volume concentration – CPVC). The refractive index of the painted layer is that one of a composite material and it is the average weighted on the volume fraction between the pigment and binder refractive indices. In this case, the painting layer was prepared by a commercial acrylic tube colour. Thermogravimetric analysis (TGA) allowed to verify that, excluding the diluents which evaporate during the film formation (about 14% of the total weight), the paint was made with about 71% in weight of acrylic binder, whose refractive index is about 1.5 at 589 nm, and 29% in weight of ivory black, whose refractive index is about 1.7 at 589 nm (ESI Fig. 1†). By considering the polymeric matrix and the inorganic phase densities, the resulting refractive index of the painting layer was about 1.58 at 589 nm. It is just an estimate since it is difficult to know the exact composition of the commercial product.

Surface roughness is an additional factor in the appearance, thus, paint layers above their CPVC or with rough surfaces are generally matte and have low colour saturation.

The application of a consolidant or varnish material on such a substrate can both lower the PVC and smooth the surface, making the paint appears more saturated and darker. On the other hand, as explained above, the maintenance of the characteristic matte appearance is necessary for some kinds of artworks.

Fig. 1a shows the appearance of the home-made matte painting-model before (Fig. 1a, Ref.) and after the application of the pristine polymer (Fig. 1a, C0), and the nanocoatings filled with an increasing concentration of titanium dioxide in the polymeric matrix (respectively, Fig. 1a, C16, C28, C44). The optical inspection of these pictures reveals that the coatings characterized by the presence of the embedded  $\text{TiO}_2$  and, as consequence, with a higher refractive index (see Table 1), appear matter and hazier with the increase of the nanoparticles concentration in the polymeric matrix, than the coating made with the pure polymer. The optical characterization of uncoated substrate and coated surfaces was performed using the FORS instrument. The samples are illuminated at  $45^\circ$  and the diffuse light collected at the surface normal (Fig. 1b). The spectra in reflectance of samples (Fig. 1c) are in good agreement with the visual appearance (Fig. 1a): the coating made with the pure

polymer (C0) is darker than the reference; in fact the colour coordinate  $L^*$ , that indicates the lightness, is 14.80 instead of 21.80. This can be attributed to the decrease of the light scattering because of the reduced substrate roughness. On the other hand, the set of films filled with  $\text{TiO}_2$  nanoparticles appears matter and hazier with the increase of nanoparticles' concentration in the polymeric matrix. This is attributed to the scattering induced by the high refractive index  $\text{TiO}_2$  particles within the paint film. In fact, the comparison between the third and fourth columns in Table 1 reveals that, although nanocomposite films are optically transparent, they show a loss in transmittance attributed to Rayleigh scattering, due to the presence of nanoparticle clusters into the polymeric matrix. In particular, the FORS spectrum of the sample characterized by the average concentration of  $\text{TiO}_2$  nanoparticles (C28) matches in the best way the reference spectrum from the reflectivity point of view. Furthermore, a feature of the films charged with titanium dioxide nanoparticles is a growth of the curve of reflectance in the blue zone of the visible range before the nanoparticles' UV absorption; it is the only difference between the reference and the sample C28 spectra and it is related to Rayleigh scattering.

In order to have a better understanding of the colour changes induced by the presence of coatings on the painted surface, the conversion of the reflectance spectra in the colorimetric coordinates  $L^*$ ,  $a^*$  and  $b^*$  has been performed.

Table 2 shows the results obtained using the CIE Standard Illuminant D65, whose spectrum is representative of the daylight condition.  $\Delta E$  values were also calculated using as reference the pristine black painted surface in order to verify whether the colour changes were effectively perceptible by human eyes.

As Table 2 shows, the only  $\Delta E$  value lower than 1.0 is related to the sample charged with the medium concentration of  $\text{TiO}_2$  in the polymeric matrix (C28). The difference of colour between the reference (Ref.) and C0 and C16 coatings is mainly attributed to the coordinate  $L^*$ , that is too low. This indicates an important decrease of the surface lightness. In fact, the paint appearance after coating with these films is too dark and saturated. On the other hand, polymeric nanocomposites show a significant difference in the colour coordinate  $b^*$  whose value shifts to lower value (blue colour) with the increase of the nanoparticles concentration in the polymer. It is related to Rayleigh scattering that mainly contributes to the diffusion of

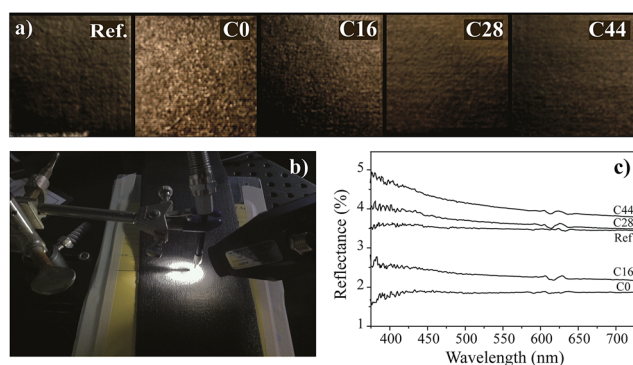


Fig. 1 (a) Images of the black painted surface before (Ref.) and after the application of the coatings: pristine poly(2-ethyl-2-oxazoline) (C0); nanocomposite films with 16 wt%, 28 wt% and 44 wt% of  $\text{TiO}_2$  in the polymeric matrix (C16, C28, C44, respectively). (b) FORS setup used to collect the spectra in reflectance of the uncoated and coated black paint. (c) FORS measurements.

Table 1 Refractive indices of the pure polymer and nanocomposite films

Coating	$\text{TiO}_2$ (%w/w)	$T$ (%) [550 nm]	$T$ (%) [694 nm]	R.I. <sup>b</sup> [550 nm]	R.I. <sup>a</sup> [694 nm]
C0	0	90.2	91.5	1.52	1.52
C16	16	88.8	90.2	1.56	1.57
C28	28	88.2	89.8	1.60	1.60
C44	44	84.7	88.4	1.67	1.65

<sup>a</sup> R.I. calculated by spectrophotometer. <sup>b</sup> R.I. measured by ellipsometer.

Table 2 Colorimetric coordinates  $L^*$ ,  $a^*$ ,  $b^*$  of the black paint (Ref.) and of the substrate coated with the pristine polymer (C0), and the films filled with  $\text{TiO}_2$  (C16, C28 and C44).  $\Delta E$  values are also reported. In bold font the only case in which  $\Delta E$  is less than 1.0, as it indicates that the change of colour is imperceptible for human eyes

	Ref.	C0	C16	C28	C44
$L^*$	21.80	14.80	17.10	22.40	23.80
$a^*$	0.02	0.2	0.1	0.1	0.09
$b^*$	-0.33	-0.25	-1.18	-1.17	-1.77
$\Delta E$	—	4.8	2	0.9	3.4



the component blue of the light. The film made with higher concentration of titanium dioxide nanoparticles (C44) scatters too much and appears lighter than the reference.

### Chemical properties, stability and reversibility of nanocoatings cast on the painting-model

Painting-replicas covered by nanocoatings were analyzed by FTIR spectroscopy before and after two years of natural aging in a conservation studio in order to verify their stability when exposed to indoor conditions.  $\text{TiO}_2$  nanoparticles are known to have photocatalytic properties and may deteriorate the polymeric matrix.<sup>39–42</sup> This could be an important drawback in the application of such a coating because it could affect its durability. On the other hand, as C. V. Horie states “the most difficult tasks of a conservator is reversing the conservation treatment of an object [...]”.<sup>43</sup> This is the reason for which this paper focuses its attention on both the assessment of the effects of the proposed material, and the possibility to remove the conservation treatment with time.

From this point of view, it is important to highlight that this research reports a proof-of-concept of protective coatings (not a ready-to-use materials) able to mimic the surface diffusive properties of some peculiar works of art, characterized by matte painted surfaces that needs to be preserved. Certainly, the proposed material cannot be used for hygroscopic paintings since it is based on an aqueous dispersion, but it could be an interesting solution for works of art sensitive to the common organic solvents (such as petroleum derivates or esters). In fact, these diluents could compromise the surface of modern and contemporary paintings made with young oils or acrylics.

The painting models are still exposed in the conservation studio, in front of a window facing west and, monitoring test will be carried out in order to evaluate the durability of the treatments after longer periods than two years.

The main IR absorption bands of the polymer poly(2-ethyl-2-oxazoline), which is a complex aliphatic tertiary amide, are reported in Table 3.<sup>44</sup> It has been reported in the literature that spectra of PEOX films, which were artificially aged under UV light ( $\lambda > 280$  nm) in a solar box, show the formation of new absorption bands of lactones and carboxylic groups ( $1730\text{ cm}^{-1}$ , C=O stretching) and of secondary amide ( $1541\text{ cm}^{-1}$ , NH bending;  $3297$  and  $3080\text{ cm}^{-1}$ , NH stretching), which are formed by oxidation and depolymerization of tertiary amide.<sup>45</sup>

By comparing the spectra in Fig. 2a of PEOX pristine polymer (C0) cast on painting-replicas, before and after natural aging, it is possible to see a new peak at  $1727\text{ cm}^{-1}$  (C=O stretching of

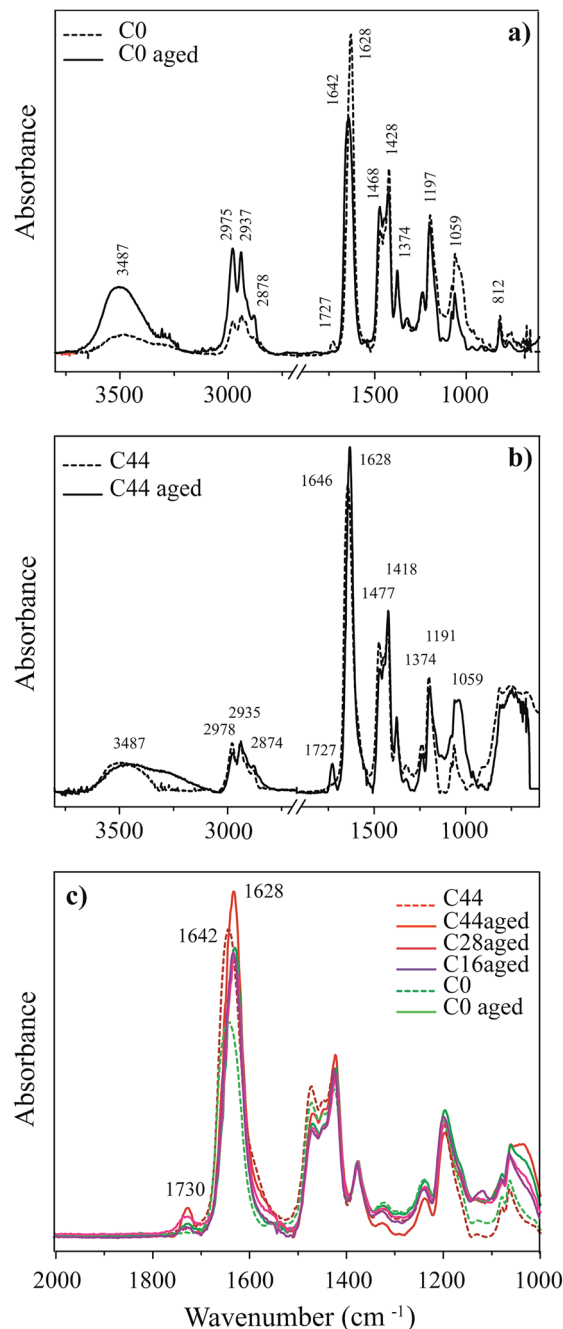


Fig. 2 (a) FTIR spectra of the C0 nanocomposite film, before (dash line) and after (dash line) a natural aging for two years. (b) FTIR spectra of the C44 nanocomposite film, before (dash line) and after (solid line) a natural aging for two years. (c) FTIR spectra of unaged C0 and C44 films and of naturally aged C0, C16, C28, C44 films.

Table 3 Main absorption bands of poly(2-ethyl-2-oxazoline)

IR bands ( $\text{cm}^{-1}$ )	Functional group
3493	NH stretching
2978, 2935, 2874	$\text{CH}_2$ , $\text{CH}_3$ stretching
1646	C=O stretching of tertiary amide
1468, 1424, 1374, 1318	CH bending
1238, 1197, 1059	C–C stretching

esters), which is indicative of the presence of oxidation products in the polymer. Moreover, the comparison between two spectra shows a decrease of the absorption bands at  $3487\text{ cm}^{-1}$ , in the region  $2878\text{--}2975\text{ cm}^{-1}$  and at  $1059\text{ cm}^{-1}$ , a shift from  $1642$  to  $1648\text{ cm}^{-1}$  of the sharp peak related to C=O stretching of tertiary amide. The absorption peaks of the acrylic painting layer have been subtracted from the spectra obtained from the replicas covered by coatings, to avoid the overlying with PEOX peaks.

In Fig. 2b, the spectrum of aged C44 nanocomposite coating shows the continuous absorption band of Ti–O starting from  $812\text{ cm}^{-1}$  and a slight increase of the peak at  $1727\text{ cm}^{-1}$ , compared to the spectra of aged C0 (Fig. 2a). As it is shown in Fig. 2c in the spectra of aged nanocoatings, by increasing the concentration of  $\text{TiO}_2$  nanoparticles, the peak at  $1727\text{ cm}^{-1}$  slightly increases but the height of this peak in C16 and C28 is comparable to that one in C0 film, indicating that, at this moment, the polymer preserves its stability, even in presence of nanoparticles.

The possibility to remove the added materials without compromising the original underlying layers has been investigated by cleaning tests on the naturally aged painting-replicas, covered by nanocomposite coatings. The complete removal of the polymer, after the treatment with TWEEN 20 and a water solution of TAC 1% w/w, has been verified by micro-FTIR Spectroscopy in  $\mu$ -ATR mode.

In Fig. 3a, the spectra of painting-model covered by C44 film, before and after the cleaning tests, and the acrylic black paint reference are reported. The absorption bands of the cleaned surfaces are perfectly overlaid with the peaks of the reference. Moreover, the spectra of the detection points of the cleaned areas do not show the continuous absorption band related to the presence of  $\text{TiO}_2$  nanoparticles ( $809\text{ cm}^{-1}$ ).

In order to better control the absence of residual  $\text{TiO}_2$  nanoparticles on the surface of the painting-model, SEM-EDX was used to obtain a semi-quantitative evaluation of the

elements (C, O, Na, Si, P, S, K, Ca, Ti) present on the surfaces of treated and cleaned painting-replicas. In Fig. 3b, the quantity of Ti in different coatings C0, C16, C28, C44, before and after the cleaning tests with TWEEN 20 and TAC is reported. As expected, the Ti content increases progressively from C0 to C44. In the cleaned areas, a complete removal of  $\text{TiO}_2$  nanoparticles occurs in C16 whereas in C28 and C44, Ti decreases but it is still present in very low amount. This can be explained by taking into account that the same cleaning treatment was used to remove every coating. Probably, for completely removing the coatings C28 and C44, the cleaning treatment should be repeated. Fig. 4 shows the morphological characterization by ESEM-EDX of the paint surface before cleaning.

The black acrylic paint reference is characterized by a rough surface where the grains of pigment are well recognizable. The application of the PEOX films makes the surface smoother, especially for painting models covered by C0 and C16 films. On the contrary, C28 coating ESEM image shows a surface, which is more similar to that of the black paint reference. Instead, C44 film presents some defects: the surface is cracked and, in some

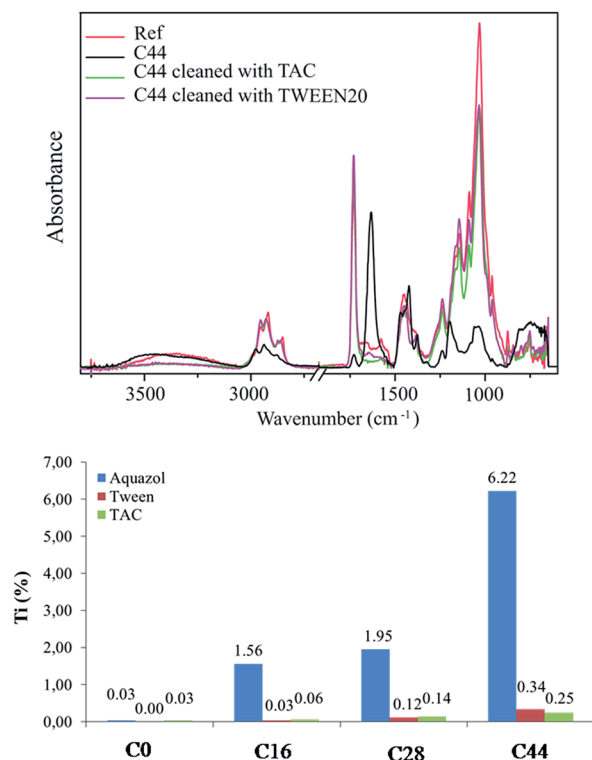


Fig. 3 (a) IR spectra before (black) and after the cleaning tests with TAC (green) and TWEEN 20 (purple) and the spectrum of the acrylic black paint reference (red). (b) Ti content (%) in C0, C16, C28, C44 coatings, before and after the cleaning tests with TWEEN 20 and TAC.

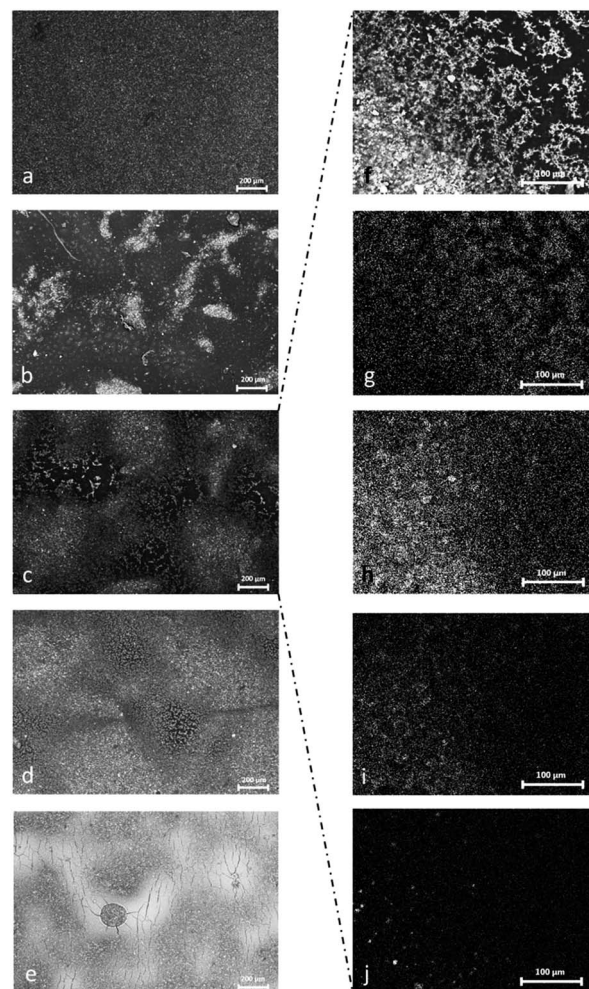


Fig. 4 ESEM-EDX characterization of the surface of aged black paint uncoated (a), and coated with nanocomposite films: C0 (b), C16 (c and f), C28 (d) and C44 films (e) and maps of distribution of the main elements Ti (g), Ca (h), P (i) and Si (j) on the C16 film (f).

areas, the film disappears. It is not clear if these defects are due to the aging or to the presence of an excessive amount of  $\text{TiO}_2$  nanoparticles in the polymer. In Fig. 4f, a SEM image at higher magnification of C16 coating is present, together with the distribution maps of the main elements (Ti, Ca, P and Si).  $\text{TiO}_2$  nanoparticles are well dispersed inside the polymeric film and the higher Ti concentration on the right part of the image is due to a higher thickness of the film. On the contrary, on the left part, the thickness of the C16 coating decreases and the characteristic signals of the underlying black paint layer (Ca, P and Si) are predominant.

### Chemical stability of nanocoatings exposed to artificial aging

In parallel to the natural aging of the painting models, artificial aging tests have been carried out by using a Xenon arc lamp as light source. Inner soda lime and borosilicate filters were used to provide daylight conditions behind a glass window. The light source spectrum presents a small portion of UV light from 300 nm to 400 nm, with an irradiance of about  $0.5 \text{ W m}^{-2}$  at 350 nm, while the major part of wavelengths owned to the visible range, with an irradiance of about  $0.9 \text{ W m}^{-2}$  at 420 nm.

Fig. 5 confirms that polyoxazolines are very stable materials; PEOX spectrum does not show any evident changes after 1517 hours.

On the other hand, C44 IR spectra (Fig. 6), collected after different times of irradiation, show important changes after only 6 hours of artificial aging. Fig. 6b shows the formation of a new band at  $1730 \text{ cm}^{-1}$  that increases with time. Moreover, after 24 hours (Fig. 6c) a shoulder of the amide carbonyl band appears at  $1670 \text{ cm}^{-1}$ , while the main peak at  $1630 \text{ cm}^{-1}$  decreases. This phenomenon continues until the carbonyl peak of the tertiary amide disappears completely (Fig. 6f). These new peaks at  $1730$  and  $1670 \text{ cm}^{-1}$  are attributed to the carbonyl functional groups of a carboxylic acid and a free secondary amide respectively. Moreover the appearance of a broad band at about  $3200 \text{ cm}^{-1}$  confirms the formation of acid hydroxyls. After 311 hours of irradiation the complete degradation of the polymer is observed.

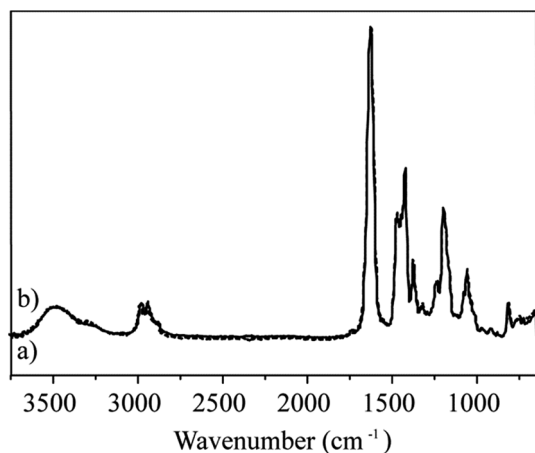


Fig. 5 Poly 2-ethyl-oxazoline (C0) spectrum after (a) 0 h and (b) 1517 h of artificial aging.

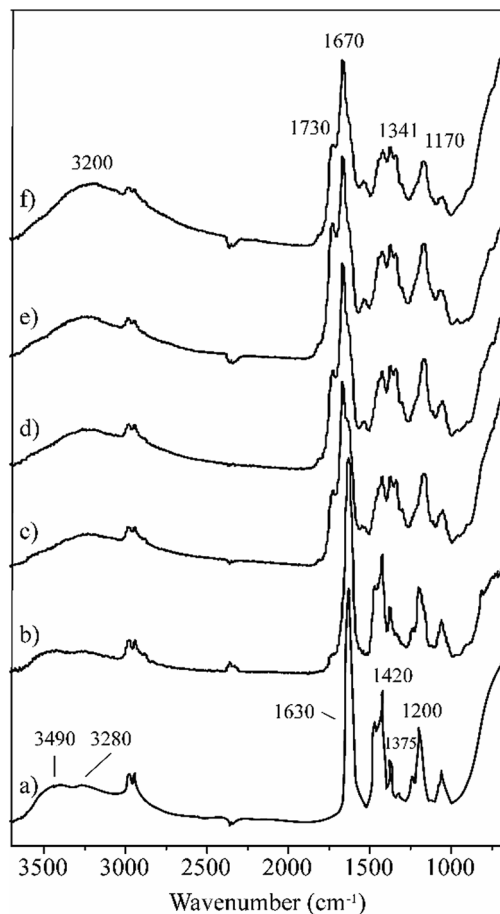
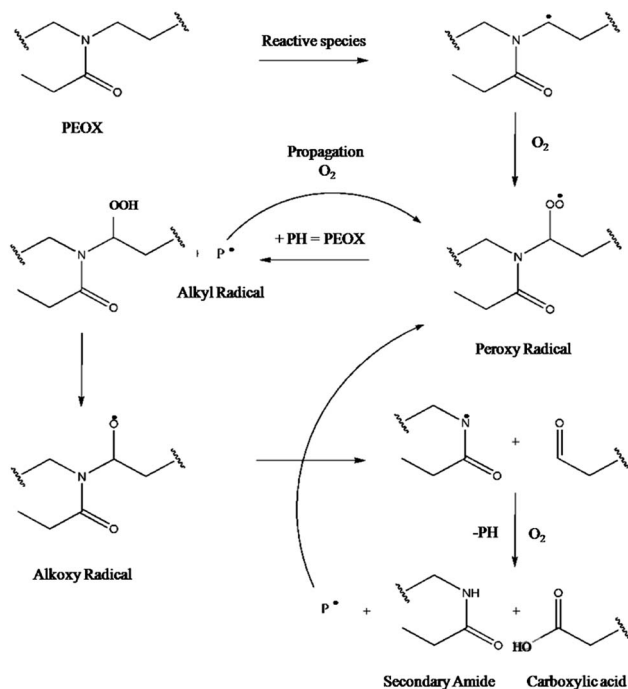


Fig. 6 FT-IR spectrum of the most concentrated nanocomposite C44 after (a) 0 h; (b) 6 h; (c) 24 h; (d) 48 h (e); 90 h and (f) 180 h of artificial aging. The spectrum of the nanocoating after 311 h is not reported here since the material is completely destroyed and no IR bands appear.

This information was used to develop and propose a mechanism of the poly(2-ethyl-2-polyoxazoline) degradation, showed in Scheme 1. The excitation of titanium dioxide by the ultraviolet light ( $\lambda < 400 \text{ nm}$ ), with the following reduction of  $\text{Ti}^{4+}$  to  $\text{Ti}^{3+}$ , in presence of oxygen, leads to the formation of oxidized reactive species such as  $\text{HO}^\bullet$ ,  $\text{H}_2\text{O}^\bullet$ ,  $\text{O}_2^\bullet$ . A conventional radical mechanism promotes the hydroperoxidation of the carbon  $\alpha$  to the nitrogen. No experimental results favour the break between the nitrogen and the carbonyl and, in that case, shorter UV wavelengths ( $\lambda < 300 \text{ nm}$  – UV-B region) are required.<sup>46–48</sup> Moreover, the attack on other carbons could not be completely ruled out. In the Scheme 1, apart from the peroxy radicals, other intermediate products are described, such as the alkyl and the alkoxy radicals, but the final result is the decomposition of the polymer in a free secondary amide and a carboxylic acid, as IR experimental data showed. This mechanism was also confirmed by GPC analysis, by observing the variation of the retention time of the polymer before and after about 44 hours of artificial aging in the weather-ometer. The pure poly(2-ethyl-2-oxazoline) preserves its pristine molecular weight with time (ESI Fig. S2†), while polymeric matrix of the higher





Scheme 1 Predicted mechanism for polyoxazoline degradation.

concentrated nanocoating shows a loss of the initial molecular weight and a consequent increase of the polydispersity after the artificial aging (ESI Fig. S3†).

This result doesn't correspond with the data obtained at the moment with natural aging, after two years of exposure behind a window facing West. It confirms that the predictive value of these tests is not absolute, as explain above. Nevertheless, artificial aging allows the introduction of a degradation mechanism of the polymeric matrix induced by the photocatalytic activity of TiO<sub>2</sub> nanoparticles, showing that the poly(2-ethyl-2-oxazoline) tends to de-polymerize instead of cross-linking, favouring its removal in future.

In fact, polymer degradation can induce two main phenomena: cross-linking and de-polymerization. The first one causes the drop of the solubility and change of the thermal properties; the second one causes the loss of the structural and optical properties of the material, but – at the same time – the preservation of the pristine solubility. In our case, coatings are soluble in aqueous systems and the solubility remains the same with time; it is a clear obviousness that the material de-polymerizes instead of cross-links.<sup>43,49</sup> The de-polymerization is a fundamental prerequisite in the conservation field since the removal of added materials in restoration treatments shouldn't compromise the pristine underlying layers and it should be possible with low aggressive systems. Clearly, aqueous methods for cleaning treatments are good for works of art that are not hygroscopic; nevertheless, to date, they are the most used in this field.<sup>50,51</sup>

Since two years are not a long time, the painting-model will be preserved and monitored for many years, in order to assess the behaviour of the nanocoatings with time.

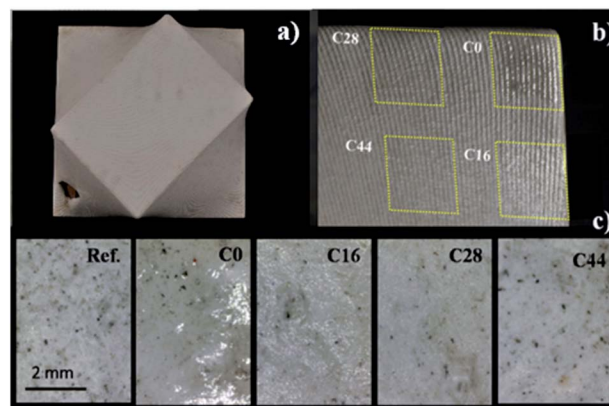


Fig. 7 (a) Photo of the white monochrome painting seen from above (before the conservation treatment); (b) test of nanocoatings brushed on the painting surface; (c) optical inspection of the treated areas by portable digital microscope.

### Application of nanocoatings on a real painting

The nanocomposite material was tested on a contemporary work of art: a model-studio made with a white colour (titanium dioxide and kaolin dispersed in a vinyl resin) cast on a double support of PVC with phthalate and cotton, attributed to Agostino Bonalumi. In this case, C44 nanocoating provides the best aesthetical compatibility by optical inspection, confirmed with portable microscope, while the areas treated with pure PEOX and the less charged nanocoatings are too glossy for an invisible preservation treatment (see Fig. 7). Table 4 shows the colorimetric coordinates  $L^*$ ,  $a^*$ ,  $b^*$  measured using the CIE Standard Illuminant D65.  $\Delta E$  values have been also calculated, using as reference the pristine white surface of every pre-treated area of the painting, in order to quantify colour changes. According to  $\Delta E$  values, C28 and C44 coatings provide the best result, even if – from inspection with a microscope – C44 seems to be more suitable from the optical point of view. The areas treated with C0 and C16 materials show visible differences from the original, mainly attributed to the coordinate  $L^*$ , that is too low, sign of a decrease of the surface lightness, and of the coordinate  $b^*$ , whose value shifts to higher value (warmer colour). This can be mainly attributed to PEOX, whose appearance is slightly yellow.

Table 4 Colorimetric coordinates  $L^*$ ,  $a^*$ ,  $b^*$  of the painting surface before and after the treatment with coatings: C0, C16, C28 and C44.  $\Delta E$  values are also reported. In bold font the cases in which  $\Delta E$  is less than 1.0, as it indicates that the change of colour is imperceptible for human eyes

	Pre-treatment			Post-treatment			$\Delta E$
	$L^*$	$a^*$	$b^*$	$L^*$	$a^*$	$b^*$	
C0	80.8	0.63	8.6	79.1	0.55	9.4	2
C16	82.8	0.36	8.1	82.3	0.29	8.9	1
C28	81.8	0.38	8.5	81.9	0.39	8.9	<b>0.4</b>
C44	83.8	0.37	8.12	83.1	0.27	8.5	<b>0.3</b>



## Conclusions

The present study reports the set-up of novel nanocoatings able to mimic the surface diffusive properties of matte painted surfaces. It has been obtained by exploiting the bulk scattering phenomenon induced by the presence of nanoparticles with tailored optical properties (high refractive index and optical transparency in the visible range), suitably dispersed in a polymeric matrix. Three different concentrations of TiO<sub>2</sub> nanoparticles dispersed in poly(2-ethyl-2-oxazoline) were prepared, obtaining transparent nanocomposites characterized by tunable optical properties. In particular, films showed UV filtering up to the proximity of the visible range and tailored refractive index, up to about 1.67, by the increasing concentration of nanoparticles in the polymeric matrix. Moreover, although nanocomposite films were optically transparent, they show a loss in transmittance attributed to Rayleigh scattering, due to the presence of nanoparticles clusters in the matrix. Thanks to the possibility to tune the amount of diffused light by the nanoparticles concentration in the polymer, a novel application of this material has been found for the treatment of matte artworks. The optical performances of this material have been tested on a black acrylic monochrome painting, in order to simulate its application in the conservation of cultural heritage. FORS measurements have been able to describe the optical appearance of the painting-replicas after the treatment with nanocoatings, revealing that is possible to match the reflective properties of the pristine painted surface by tailoring the amount of nanoparticles in the polymeric matrix *via* bulk scattering. Moreover, the increase of the nanoparticles concentration in the polymeric matrix can provide a weak increase of the surface roughness, whose specific contribution to the light scattering has not been evaluated.

The requirement of stability and reversibility of this material cast on painting models has been checked after two years of natural aging. FTIR measurements showed a weak aging of the polymer revealing that, in natural indoor conditions, TiO<sub>2</sub> nanoparticles does not cause extensive degradation. On the other hand, artificial aging tests showed that TiO<sub>2</sub> nanoparticles can catalyze de-polymerization of the poly(2-ethyl-2-oxazoline) over time, with the important consequence that the polymer will remain soluble in organic and aqueous solvents.

This has been demonstrated for the naturally aged sample by the dissolution of the material with aqueous solutions added with a non-ionic surfactant (TWEEN 20) and a weak chelate agent (ammonium citrate tribasic). The removal efficacy was ascertained by FTIR and SEM-EDX measurements on micro-samples taken away from the painted surfaces, in which we showed that it is possible to almost completely remove both the polymer and TiO<sub>2</sub> nanoparticles.

The results in terms of optical compatibility and retreatability obtained in this simulated painting suggested that this material is a promising proof of concept for the consolidation of matte artworks. For all these reason, it has been already tested with good result, from the optical point of view, during

a restoration treatment of a real contemporary work of art characterized by important conservation problems, attributed to the Italian artist Agostino Bonalumi. The stability of TiO<sub>2</sub> nanocoatings should be further investigated as well as the possibility of using less photo-active nanoparticles. From this point of view, the best approach could be to cover the TiO<sub>2</sub> nanoparticles surface with a shell of SiO<sub>2</sub> and Al<sub>2</sub>O<sub>3</sub>, that are inert, transparent in the visible range, and characterized by a refractive index close to the polymeric matrix (1.46 at 589 nm for silicon dioxide and about 1.77 at 589 nm for alumina). Moreover, there are some examples in literature involved in the development of core-shell TiO<sub>2</sub>-SiO<sub>2</sub> and TiO<sub>2</sub>-Al<sub>2</sub>O<sub>3</sub> nanoparticles.<sup>52</sup>

## Acknowledgements

We thank Carlotta Beccaria and Valentina Mombrini by the conservation studio Carlotta Beccaria & C. S.a.s. in Milano for the restoration activity on the painting-replicas and the model-studio painting attributed to A. Bonalumi.

## Notes and references

- 1 E. R. de la Rie, J. K. Delaney, K. M. Morales, C. A. Maines and L. Sung, *Stud. Conserv.*, 2010, **55**, 134.
- 2 J. K. Delaney, E. R. de la Rie, M. Elias, L. Sung and K. M. Morales, *Stud. Conserv.*, 2008, **53**, 170.
- 3 E. R. de la Rie, *Stud. Conserv.*, 1987, **32**, 1.
- 4 M. Ambrosi, L. Dei, R. Giorgi, C. Neto and P. Baglioni, *Langmuir*, 2001, **17**, 4251.
- 5 R. Giorgi, L. Dei, M. Ceccato, C. Schettino and P. Baglioni, *Langmuir*, 2002, **18**, 8198.
- 6 R. Giorgi, C. Bozzi, L. Dei, C. Gabbiani, B. W. Ninham and P. Baglioni, *Langmuir*, 2005, **21**, 8495.
- 7 G. Poggi, R. Giorgi, N. Toccafondi, V. Katzur and P. Baglioni, *Langmuir*, 2010, **26**, 19084.
- 8 D. Chelazzi, G. Poggi, Y. Jaidar, N. Toccafondi, R. Giorgi and P. Baglioni, *J. Colloid Interface Sci.*, 2013, **392**, 42.
- 9 D. L. Scarlone and O. Chiantore, *Polym. Degrad. Stab.*, 2012, **97**, 2136.
- 10 C. Kapridaki and P. Maravelaki-Kalaitzaki, *Prog. Org. Coat.*, 2013, **76**, 400.
- 11 P. N. Manoudis, I. Karapanagiotis, A. Tsakalof, I. Zuburtikudis, B. Kolinkeová and C. Panayiotou, *Appl. Phys. A*, 2009, **97**, 351.
- 12 E. Quagliarini, F. Bondioli, G. B. Goffredo, A. Licciulli and P. Munafò, *J. Cult. Herit.*, 2013, **14**, 1.
- 13 A. Licciulli, A. Calia, M. Lettieri, D. Diso, M. Masieri, S. Franza, R. Amadelli and G. Casarano, *J. Sol-Gel Sci. Technol.*, 2011, **60**, 437.
- 14 M. Afsharpour, F. T. Rad and H. Malekian, New cellulosic titanium dioxide nanocomposite as a protective coating for preserving paper-art-works, *J. Cult. Herit.*, 2011, **12**(4), 380.
- 15 E. D. Palik and G. Gosh, *Handbook of optical constants of solids*, Academic Press, San Diego, 1998.
- 16 K. M. Noone, N. C. Anderson, N. E. Horwitz, A. M. Munro, A. P. Kulkarni and D. S. Ginger, *ACS Nano*, 2009, **3**, 1345.

- 17 D. Kuang, J. Brillet, P. Chen, M. Takata, S. Uchida, H. Miura, K. Sumioka, S. M. Zakeeruddin and M. Grätzel, *ACS Nano*, 2008, **2**, 1113.
- 18 H. Zhang, G. Chen and D. W. Bahnemann, *J. Mater. Chem.*, 2009, **19**, 5089.
- 19 M. Pelaez, P. Falaras, A. G. Kontos, A. A. de la Cruz, K. O'shea, P. S. M. Dunlop, J. A. Byrne and D. D. Dionysiou, *Appl. Phys. A*, 2012, **121–122**, 30.
- 20 W. Y. Youngblood, S. A. Lee, K. Maeda and T. E. Mallouk, *Acc. Chem. Res.*, 2009, **42**, 1966.
- 21 H. Althues, J. Henl and S. Kaskel, *Chem. Soc. Rev.*, 2007, **36**, 1454.
- 22 A. Colombo, F. Tassone, F. Santolini, N. Contiello, A. Gambirasio and R. Simonutti, *J. Mater. Chem. C*, 2013, **1**, 2927.
- 23 R. J. Nussbaumer, W. R. Caseri, P. Smith and T. Tervoort, *Macromol. Mater. Eng.*, 2003, **288**, 44.
- 24 S. Lee, H. J. Shin, S. M. Yoon, D. K. Yi, J. Y. Choi and U. Paik, *J. Mater. Chem.*, 2008, **18**, 1751.
- 25 M. M. Demir, K. Koynov, Ü. Akbey, C. Bubek, I. Park, I. Lieberwirth and G. Wegner, *Macromolecules*, 2007, **40**, 1089.
- 26 X. Chen, S. Shen, L. Guo and S. S. Mao, *Chem. Rev.*, 2010, **11**, 6503.
- 27 C. Lü and B. Yang, *J. Mater. Chem.*, 2009, **19**, 2884.
- 28 T. T. Chiu, B. P. Thill and W. J. Fairchok, Poly(2-ethyl-2-oxazoline): A New Water- and Organic-Soluble Adhesive, in *Water-Soluble Polymers*, American Chemical Society, 1986, ch. 23, p. 425.
- 29 G. Mueller and S. Ahmes, Moisture-activable adhesive reinforcement strings and tear opening tapes for corrugated and cartonstock containers, *US Pat.*, 7041194 B1, 1999.
- 30 J. Arslanoglu and C. Tallent, *Evaluation of the Use of Aquazol as an Adhesive in Paintings Conservation*, Western Association for Art Conservation (WAAC), 2003, vol. 25, p. 12.
- 31 J. Arslanoglu, Using Aquazol: A Brief Summary, *American Institute for Conservation of Historic and Artistic Works Paintings Specialty Group*, 2005, p. 107.
- 32 V. Muros, Investigation into the Use of Aquazol as an Adhesive on Archaeological Sites, *WAAC Newsletter*, 2012, **34**, 9.
- 33 M. Niederberger, M. H. Bartl and G. D. Stucky, *Chem. Mater.*, 2002, **14**, 4364.
- 34 A. Colombo, F. Tassone, M. Mauri, D. Salerno, J. K. Delaney, M. R. Palmer, R. de La Rie and R. Simonutti, *RSC Adv.*, 2012, **2**, 6628.
- 35 G. Thomson, *The museum environment*, Butterworth-Heinemann, London, UK, 1986, p. 293.
- 36 D. Franta and I. Ohlidal, *J. Mod. Opt.*, 1998, **45**, 903.
- 37 H. J. Porck and J. Henk, *European Commission on Preservation and Access. Rate of paper degradation: the predictive value of artificial aging tests*, European commission on preservation and access, Amsterdam, 2000.
- 38 C. Amra, *Appl. Opt.*, 1993, **32**, 5481–5491.
- 39 X. Chen and S. S. Mao, *Chem. Rev.*, 2007, **107**, 2891.
- 40 A. Fujishima, T. N. Rao and D. A. Tryk, *J. Photochem. Photobiol., C*, 2000, **1**, 1.
- 41 A. Fujishima and X. Zhang, *C. R. Chim.*, 2006, **9**, 750.
- 42 A. Fujishima, X. Zhang and S. A. Tryk, *Surf. Sci. Rep.*, 2008, **63**, 515.
- 43 C. V. Horie, *Materials for Conservation-Adhesives, consolidants and lacquers*, Butterworths, 1987.
- 44 R. C. Wolbers and M. D. McGinn, *Poly(2-Ethyl-2-Oxazoline): a new conservation consolidant in Symposium: Painted Wood, History and Conservation*, Getty Conservation Institute, Los Angeles, 1994.
- 45 M. Camaiti, L. Borgioli and L. Rosi, *Chim. Ind.*, 2011, 100.
- 46 L. Tang, D. Sallet and J. Lemaire, *Macromolecules*, 1982, **15**, 1432.
- 47 P. Cerruti, M. Lavorgna, C. Carfagna and L. Nicolais, *Polymer*, 2005, **46**, 4571.
- 48 R. Konradi, C. Acikgoz and M. Textor, *Macromol. Rapid Commun.*, 2012, **33**, 1663.
- 49 M. R. Kamal and B. Huang, Natural and artificial weathering of polymers, in *Handbook of Polymer Degradation*, ed. S. H. Hamid, M. B. Ami and A. G. Maadhan, Marcel Dekker, New York, NY, 1992, pp. 127–168.
- 50 R. Wolbers, *Cleaning Painted Surfaces, Aqueous Methods*, Archetype, London, 2000.
- 51 M. Baglioni, R. Giorgi, D. Berti and P. Baglioni, *Nanoscale*, 2012, **4**, 42.
- 52 N. S. Allen, M. Edge, A. Ortega, G. Sandoval, C. M. Liauw, J. Verran, J. Stratton and R. B. McIntyre, *Polym. Degrad. Stab.*, 2004, **85**, 927.